21st century changes in snow w~~W~~ater e~~E~~quivalent over Northern Hemisphere landmasses due to increasing temperature, projected with the CMIP5 m~~M~~odels

By

H. X. Shi and C. H. Wang

Key Laboratory of Arid Climate Change and Disaster Reduction of Gansu Province,

College of Atmosphere Science, Lanzhou University, Lanzhou, China, 730000

Changes in snow water equivalent (SWE) over Northern Hemisphere (NH) landmasses are investigated for the early (2016−2035), middle (2046−2065) and late (2080−2099) 21st century using twenty global climate models~~, which are~~ from the Coupled Model Intercomparison Project Phase 5 (CMIP5). ~~The results show that, relative to the 1986–2005 mean~~, T~~t~~he multi-model ensemble projects a significant decrease in SWE for most regions relative to the 1986–2005 mean under three Representative Concentration Pathways (RCP), This decrease is particularly evident~~particularly~~ over the Tibetan Plateau and western North America, whereas ~~but~~ an increase occurs over~~in~~ eastern Siberia. Seasonal SWE projections show an overall decreasing trend, with the greatest reduction in spring, which is linked to the stronger inverse partial correlation between the SWE and increasing temperature. The largest relative reduction in SWE over the NH does not occur in spring but in summer. ~~Moreover,~~ Z~~z~~onal mean annual SWE exhibits

significant reductions for ~~in~~ RCPs~~three Representative Concentration Pathways(RCP)~~, and the magnitude of the reduction gradually decreases with latitude in the NH from south to north. A~~a~~ stronger linear relationship between SWE and temperature at mid–high latitudes suggests the reduction in SWE there is related to rising temperature. As temperature increases, the reduction in the fraction of solid precipitation becomes the main contributor to the change in SWE from August to May in the next year in the 21st century, and after May the reduction in SWE is controlled primarily by the decrease in accumulated snowfall. In summary, our results show a trend towards decreasing SWE, and the decreases in solid precipitation and accumulated snowfall strongly affect the change in SWE before and after May, respectively. ~~However, the rate of reduction in SWE declines gradually during the 21st century, indicating that the temperature may reach a threshold value that decreases the rate of SWE reduction. A large reduction in zonal maximum SWE (ZMSWE) between 30° and 40°N is evident in all 21st century for the three RCPs, while RCP8.5 alone indicates a further reduction at high latitudes in the late period of the century. This pattern implies that ZMSWE is affected not only by a terrain factor but also by the increasing temperature. In summary, our results show both a decreasing trend in SWE in the 21st and a decline in the rate of SWE reduction over the 21st century despite rising temperatures.~~

Key words: Coupled Model Intercomparison Project (CMIP5); Snow Water Equivalent (SWE); Model assessment and projection; Sensitivity

1 Introduction

Snow is ~~As~~ a key component of the cryosphere, ~~snow~~ and plays a fundamental role in global climate~~,~~ due to its high albedo and cooling effect (Vavrus, 2007). However, ~~as global temperatures increase,~~ terrestrial snow cover in the Northern Hemisphere (NH) is changing rapidly alongside increasing global temperatures. According to the IPCC Fifth Assessment Report (AR5) (IPCC, 2013) NH snow cover extent decreased by 1.6 [0.8 to 2.4]% per decade for March and April, and by 11.7 [8.8 to 14.6]% per decade for June, during the period 1967–2012. Furthermore, the projections show a 7% decrease in the total area of NH spring snow cover for Representative Concentration Pathway (RCP) 2.6 and a 25% decrease for RCP8.5 by the end of the 21st century. This result is consistent with results from the IPCC Fourth Assessment Report (AR4) (IPCC, 2007). Projections of mean annual NH snow cover suggest a further 13% reduction by the end of the 21st century under the B2 scenario, with individual projections ranging from 9% to 17%; i.e., despite different emission scenarios, the change in snow cover over the NH land shows the same decreasing trend. ~~According to the IPCC Third Assessment Report (TAR) (Houghton et al., 2001), the total area of snow-covered land in the NH has decreased by ~10% since the 1960s. Meanwhile, projections of mean annual NH snow cover suggest a further 13% reduction by the end of the 21st century under the B2 scenario, with individual projections ranging from 9% to 17% (Meehl et al., 2007). Furthermore, according to the IPCC Fifth Assessment Report (AR5) (Stocker et al., 2013), the total area of NH spring snow cover will decrease by 7% for Representative Concentration Pathway (RCP) 2.6 and by 25% for RCP8.5 by the end of the 21st century. From TAR to AR5, although the models' scenarios are different, the area of NH snow cover all represents a declined trend, owing to the fact that snow is highly sensitive to rising temperature.~~

~~Indeed,~~ S~~s~~everal studies have shown that marked decreases in the area and/or depth of snow have already occurred in regions such as western North America (Groisman et al., 2004; Stewart et al., 2005), central Europe (Falarz, 2002; Vojtek et al., 2003; Scherrer et al., 2004) and China (Ji et al., 2012; Wang et al., 2012), thus highlighting the need for better projections of future snow conditions.

Snow cover represents a spatially and temporally integrated response to snowfall events (Brown and Mote, 2009), and may have a direct relationship with temperature (Brutel-Vuilmet et al., 2013). Snow depth mainly reflects the magnitude of precipitation (snowfall), whereas snow water equivalent (SWE) primarily reflects the combined impact of temperature and precipitation (Räisänen, 2008).~~The snow depth mainly represents the magnitude of precipitation (snowfall) (Räisänen, 2008), snow cover possibly exhibit a more direct relationship to temperature (Brutel-Vuilmet, 2013). However~~whereas~~,~~ snow water equivalent (SWE) primarily reflects the ~~common~~ combined impact of temperature and precipitation on snow (Räisänen, 2008). According to AR5 (~~Stocker et al.~~IPCC, 2013), ~~the~~ global temperature and precipitation will ~~persistently~~ increase in the 21st century. The dependence of global warming on the RCP emission pathway is weak for the next few decades but strengthens rapidly towards the end of this century (IPCC, 2013).~~,~~ Of primary concern is the way that SWE will respond to changes in temperature and precipitation. AR5 reported that SWE responds to both temperature and precipitation, and is more sensitive to the snowfall amount at the beginning and end of the snow season (IPCC, 2013).~~in order to study the influence of temperature and precipitation on snow, SWE is arguably the most effective tool for assessing the hydrologic impact of snow cover variability (Bulygina et al., 2009), owing to the large number of studies to date. For example, SWE measurements from northwest North America were described by Clark et al (2001) and have since been used by McCabe and Dettinger (2002) to improve forecasting of seasonal streamflow. Following comparison with observational data,~~

G~~g~~lobal climate models consistently project declining SWE in many areas by the end of 21st century, while some models shows an increase in snowpack along the Arctic Rim by 2100 (Hayhoe et al., 2004; Brown and Mote, 2009). For example, a 20 km-mesh atmospheric general circulation model projects decreased SWE over much of the NH, and increased SWE over colder regions (Siberia and northernmost North America) due to increasing snowfall during the coldest ~~seasons~~months~~, although the percentage change of SWE depend on geographical features~~ (Hosaka et al., 2005). Brutel-Vuilmet et al. (2013) also indicated that the greatest relative reduction in maximum SWE at low latitudes is related to decreasing snowfall. ~~Similarly, a regional climate simulation for North America reported increased March SWE in parts of Alaska and Arctic Canada, but decreasing values farther south (Christensen et al., 2007).~~

Räisänen (2008) suggested that changes in seasonal SWE by the end of the 21st century will vary regionally and depend on local climate conditions. ~~According to the Coupled Model Intercomparison Project Phase 3 (CMIP3) projections, changes in seasonal SWE by the end of the 21st century will be spatially variable, with much depending on present local climate conditions (Räisänen, 2008). For example,~~ I~~i~~n very cold regions, for example ~~climate~~ warming will lead to greater winter snowfall, and thus a thicker snowpack, whereas in warm regions, higher temperatures will result in reduced snowfall. Similarly, CMIP5 experiments project declining SWE over North America south of 70°N (concentrated over the Rocky Mountains, to southern Alaska, and the eastern Canadian provinces), with maximum changes during the peak snow season (January−April), and increasing SWE north of 70°N due to enhanced precipitation (Maloney et al., 2012). ~~Except the influence of climate factor on SWE, Topography also influences variability in SWE.~~ In the mountainous regions of Europe and western North America, projected reductions in SWE are greatest at low elevations (Maloney et al., 2012).~~,~~ SWE is generally projected to decrease less with increasing altitude due to colder winter conditions,~~but decreases less with increasing altitude, owing to colder winter conditions,~~ while in some areas, simulated SWE actually increase with altitude (Scherrer et al., 2004; Mote et al., 2005; Mote, 2006). ~~Namely, the changes in SWE vary with the altitude.~~

According to AR5 (~~Stocker et al.~~IPCC, 2013), anthropogenic warming will continue beyond 2100 for all RCPs, ~~with the consequences of~~leading to an accelerationn~~ng~~ of the water cycle and a changing ~~the~~ ratio of snowfall to rainfall. Moreover, increased winter precipitation likely will be insufficient to offset the greater contribution of liquid precipitation and enhanced snowmelt driven by higher average temperatures (Räisänen and Eklund, 2011~~, 2011~~). From TAR to AR5, projected linear trends in SWE under different scenarios are highly variable since SWE is dependent both on the concentration of total emissions and the duration of emissions.

The above studies show that changes in SWE generally depend on both temperature and precipitation, but their relative contributions remain debated. ~~Furthermore,~~ S~~s~~everal studies have concluded that increasing temperature plays a major role in decreasing SWE (Lemke et al., 2007; Räisänen and Eklund, 2011), whereas other studies indicate that increasing SWE is mainly related to increasing precipitation (Hosaka et al., 2005; Maloney et al., 2012). Räisänen (2008) suggested that changes in SWE depend on the competing influences of temperature and precipitation; i.e., an increase in precipitation, if acting alone, would lead to an increase in snowfall and consequently to increased amounts of snow on ground, while an increase in temperature alone would reduce the fraction of precipitation that falls as snow and increase snow melt.~~SWE variability can be attributed to either increasing precipitation (Hosaka et al., 2005; Maloney et al., 2012) or temperature (Lemke et al., 2007; Räisänen, 2011), while Räisänen (2008) suggested that the cryospheric response depends on the balance between increasing temperature and precipitation~~. Consequently, ~~our~~ the present study was motivated by the need to address the following questions: (1) ~~Throughout the NH scale,~~ how will NH

SWE respond to the different RCPs ~~projected for~~in the 21st century? (2) How will the relationships between SWE and temperature, and between SWE and precipitation change during different periods of the 21st century?~~about the link between SWE and climate change?~~

To further analyze anticipated changes in SWE, we employed output from the CMIP5 models in conjunction with GlobSnow product. ~~Here,~~ W~~w~~e focus primarily on temporal and spatial changes in SWE and on variations in the relationship between SWE and climate for each RCP during different periods of ~~in the~~ 21st century. The specific datasets used in this study are described in Section 2, and the simulated and observed data are compared ~~and the comparison between simulated and observed dataset are given~~ in Section 3. Temporal and spatial characteristics of SWE are projected and analyzed in Section 4, and the relationships between SWE and climate change are discussed in Section 5. The key findings of the study~~The main results~~ are summarized in Section 6

2 Datasets

To objectively quantify the changes of SWE in the 21st century, we examined 20 models participating in CMIP5 (Table1), those models –all provide monthly SWE ~~variable~~ in ~~the~~ historical experiment and three scenarios experiments (RCP2.6, RCP4.5 and RCP8.5), and we only use the first ensemble member produced by each model (e.g., r1i1p1). While these models vary in their forcing parameters, each model includes ~~the~~ an increases in major anthropogenic aerosols observed during ~~the~~ 1850-2005 and anticipated for the future scenarios. Further details ~~are given~~can be found at http://www-pcmdi.llnl.gov.

The model simulations ~~of the models~~ cover the periods 2006−2099 and 2006−2300. Here, we describe changes in SWE during the former period, which is divided into three ~~segments~~sub-periods: the early (2016−2035: EP), middle (2045−2065: MP) and late (2080−2099: LP) 21st century. The analyses were conducted using a 1°×1° latitude–longitude grid, and re-gridding of original model grids ~~to the analysis grids~~ was conducted via bilinear interpolation.

To verify the performance of the CMIP5 models for simulating SWE, we compare~~d~~ the CMIP5 output with the monthly SWE data from European Space Agency (ESA) GlobSnow dataset (Takala et al., 2011). GlobSnow combines SWE retrieved from passive microwave~~ observation~~ and weather station observation. This is the most realistic SWE product currently available (Hancock et al., 2013) because of the improved accuracy achieved by assimilating independent sources of information~~Because of the improved accuracy achieved by assimilating independent sources of information, this is a more realistic SWE product currently available (Hancock et al., 2013)~~. The series cover the period of 1979-2010 ~~, and the SWE data have~~with a resolution ratio of 25×25 km, and is also interpolated onto a common 1°×1° grid. Hereafter, we refer to the GlobSnow dataset as the observed SWE.

In this paper, linear correlation coefficients, partial correlation analysis and regression analysis are used to investigate the relation between model simulations from different scenario experiments and observations. The equations are as follows.

Partial correlation:

$$r_{XY,Z} = \frac{r_{XY} - r_{XZ} r_{YZ}}{\sqrt{(1 - r_{XZ}^2)(1 - r_{YZ}^2)}} \quad (1)$$

where $r_{XY,Z}$ indicates the contribution of *X* to *Y*, after removing the contribution of *Z* to *Y*.

Regression coefficient:

$$Y = b + at \quad (2)$$

where *a* represents the linear trend of factor *Y* with time *t*.

Relative-error ratio (RE):

$$RE = \frac{S_i - O_i}{O_i} \times 100\% \qquad (3)$$

where *RE* reflects the change in a variable *S* relative to the baseline *O*.

Räisänen (2008) suggested that the change in SWE (ΔSWE) can be decomposed into four terms:

$$\Delta SWE = \underbrace{\overline{G}\int \overline{F}\Delta P dt}_{\Delta SWE(\Delta P)} + \underbrace{\overline{G}\int \Delta F \overline{P} dt}_{\Delta SWE(\Delta F)} + \underbrace{\Delta G\int \overline{F}\,\overline{P} dt}_{\Delta SWE(\Delta G)} + \underbrace{\frac{1}{4}\Delta G\int \Delta F \Delta P dt}_{\Delta SWE(NL)} \qquad (4)$$

where the first three terms on the right represent the contribution from changes in total precipitation (ΔP), fraction of solid precipitation (ΔF) and the fraction of accumulated snowfall that remains on the ground (ΔG). $\Delta SWE(NL)$ is a non-linear combination of ΔG, ΔF and ΔP. P_1 is mean total precipitation during different periods of the 21st century, and P_0 is the mean total precipitation during 1986–2005. $\overline{P} = (P_0 + P_1)/2$, $\Delta P = (P_1 - P_0)$, the definitions of $\overline{G}, \Delta G, \overline{F}, \Delta F$ can refer to $\overline{P}, \Delta P$

3 Validation of CMIP5 simulations for SWE

To evaluate the simulation performance of the models used in this study, we calculated spatial correlations and standard deviation ratios for the observed and simulated winter (DJF) mean SWE (Fig.~~ure~~ 1). ~~We found that each~~ simulated SWE from each model exhibits a strong~~close~~ spatial correlation (~~P~~*p*<0.05) with ~~the~~ observations, and ~~the majority of~~most standard deviation ratios are close to one. ~~By comparison, most existing models have less-robust correlations and lower standard deviation ratios with the observed data in the time series from 1980 to 2005. However,~~ These results indicate that the models can reproduce the spatial characteristics of SWE. Furthermore, the multi-model ensembles can ~~evidently~~ improve simulation ~~the~~ performance, ~~which~~ and has~~ve~~ better correlation and standard deviation ratios than ~~the~~ most individual model. ~~In addition,~~ Fig.2 shows both the observed and the simulated ~~averaged~~ mean winter ~~mean~~ SWE over ~~the Northern Hemisphere~~NH land covered by the GlobSnow data. ~~is also shown in Fig. 2~~. The observed ~~average~~ mean winter ~~mean~~ SWE over ~~the northern Hemisphere~~NH is 71.6 kg m^{-2}, while the stimulation ranges from 61.0 to 111.3 kg m^{-2}. The RE ranges from −20.3% to 55.4%. ~~Significantly,~~ M~~m~~ost models overestimate SWE, and only five models (CanESM2, CSIRO-Mk3-6-0, HadGEM2-ES, MPI-ESM-LR, MPI-ESM-MR) underestimate SWE, with a RE of −20% to −0.4%. ~~compared with the observation,~~ However, ~~and~~ the multi-model mean is 80.8 kg m^{-2}, which is closer to ~~the~~ observation than ~~the~~ most of the individual model. This illustrates that the multi-model ensemble is more effective for simulating changes in SWE than individual models. From here on, all simulation values ~~denote~~ are from the multi-model means, and we take the period of 1986-2005 from the ~~in~~ historical experiment (1850-2005) as the reference period.

4 Changes in SWE in the 21st century

~~In order~~ T~~t~~o project future spatial and temporal SWE patterns, we analyze three simulatons ~~of SWE change, we analyze simulations for the three RCPs~~ (RCP2.6, RCP4.5, RCP8.5) ~~on temporal and spatial scales~~.

4.1 Spatial changes in SWE for ~~the~~ three RCPs

~~General patterns of~~ P~~p~~rojected spatial changes in SWE relative to 1986-2005 (RP) for the three periods of the 21st century are shown in Fig. 3. ~~Relative to the reference period 1986–2005 (RP),~~The mean annual SWE declines over much of the NH for all the RCPs, with the greatest changes occurring over the Tibetan Plateau (TP);~~.~~ the multi-model mean decrease in SWE exceeds 80% in the western TP. The only regions ~~Only~~ where a weak increase in SWE (RE < 20%) is observed are ~~in~~ eastern Russia and Siberia ~~does a weak increase in SWE occur~~. Over North America, ~~above~~ north of 60°N, ~~we observed~~ there is a pronounced reduction in SWE during the LP for RCP8.5~~,~~ with an ~~relative error ratios (~~RE~~)~~ that rang~~s~~ing from -40% to -10%.~~,~~

~~and from -20% to -10%~~ F~~f~~or both RCP2.6 and RCP4.5, the RE ranges from -20% to -10%. In contrast, i~~I~~n eastern Siberia~~,~~ the RE ~~increases to~~is from 10% to ~~≈~~20% for RCP8.5, while for both RCP2.6 and RCP4.5 the RE is <~~less than~~ 10%. This distribution suggests that the magnitude of the SWE decrease (increase in Siberia) gradually becomes larger with time and with higher emissions. ~~This pattern suggests that, as emissions rise, the intensity of decreased or increased SWE both increases. Meanwhile, we note that the decline in SWE is greater during the LP than during the EP and MP for the same emission scenario.~~

The changes in SWE in winter and spring (not shown) ~~Simulations of mean annual SWE~~ show a similar pattern to ~~those~~ that of mean annual SWE.~~winter and spring (not shown). For example,~~ I~~i~~n springtime, for example, the RE ~~of SWE~~ is between -20% and -10% over northern North America and ranges from -40% to -20% over most of Europe. In Siberia, the multi-model mean increase in SWE exceeds 10%. Over the whole NH, t~~T~~he extent of increased springtime SWE (RE > 0) is comparable to that ~~basically the same as that~~ in winter and for the annual mean. Nonetheless, the magnitude of decline of SWE in spring exceeds that in ~~other seasons~~winter so that ~~, resulting that~~ the decrease ~~of~~ in SWE in spring is ~~the~~ more~~st~~ significant than that in winter.

带格式的：制表位： 33.08 字符，左对齐

As global temperatures rise, the projected reduction in SWE is most pronounced along the southern limits of seasonal snow cover. This is p~~P~~articularly apparent over the TP, ~~where is the~~a unique cold, high-altitude region ~~in the mid-latitude NH~~ (Fig. 3), where the increase in temperature is more rapid than in other mid-latitude areas (Liu, 2000; Chen, 2006; Wang et al., 2012), atmospheric warming serves to accelerate snowmelt and reduce total snowfall amounts ~~(Räisänen, 2008)~~.

~~To investigate the zonal changes in SWE,~~ Figure 4 illustrates the relative zonal changes in mean ~~-~~annual SWE, precipitation and the absolute change in temperature ~~and maximum SWE and temperature~~ derived from the multi-model ~~simulations~~ mean for the three periods of the 21st century. For all variables, the temporal trends in the multi-model mean are roughly similar in different RCPs during the same period. However, the magnitude of changes in mean annual SWE, precipitation and temperature increase with emissions (RCP) and with time.

The decrease in SWE is small in the 60–70°N latitude band for all three RCPs throughout the 21st century (RE < 30%), and the magnitude of decrease in SWE gradually declines from south to north (north of 60°N), namely, the largest relative reduction in SWE occurs at the low latitude. However, the largest absolute change in SWE (not shown) appears in the high latitudes (70−80°N). Relative to the RP, the magnitude of reduction in NH SWE gradually increases over time with increased emissions. During the LP, the absolute decrease in SWE reaches −28.0 kg m^{-2} for RCP2.6, −55.7 kg m^{-2} for RCP4.5 and −77.6 kg m^{-2} for RCP8.5.

Figure 4 d–f shows that ~~Relative to RP, the projected temperature increase by the end of the 21st century will not exceed 2°C for the lower emissions pathway (RCP2.6) (Stocker et al., 2013). However, as indicated by Fig. 4 (c, f, i),~~ temperatures will increase more rapidly at high latitude than at lower latitude. AR5 also shows that anthropogenic warming will be more pronounced at high latitudes (IPCC, 2013). The temperature increase is greater over time and with higher emissions (RCP), and temperature increases more rapidly in the 50–60°N latitude band than in other areas. The temperature increase does not exceed 2°C in RCP2.6 by the end of the 21st century, which is in agreement with the results of AR5 (IPCC, 2013). Similarly, a greater increase in precipitation occurs in tropical and high-latitude regions during the EP, MP and LP for all three RCPs (Figure 4g–i). The minimum increase in precipitation occurs in the 30–40°N latitude band, which is likely related to the fact that most arid regions in the NH are located in this region. During the EP, relative changes in precipitation are the same for all three RCPs, but these grow larger with time and increased emissions. During the LP, the increase in precipitation exceeds 30% for RCP8.5 at high-latitudes

(70–80°N) whereas changes for the mid–low emission scenarios (RCP2.6, RCP4.5) are generally less than 20%.~~Viewed in greater detail, the model results are similar for all three RCPs during the EP, but diverge during the MP and LP. The maximum simulated increase in temperature occurs at high latitude during the LP for RCP8.5.~~

~~For all three RCPs, the simulations of mean annual SWE exhibit a clear decline throughout the 21st century (Figure 4 b, e, h), with the greatest reductions occurring at high latitudes (~70–80°N). Relative to RP, the decline in low-latitude SWE during the EP is minor (~ -10 kgm^{-2}) for all three RCPs, and the magnitude of the decline rises with increasing latitude. In contrast, the magnitude of the decline in SWE reaches -30 kg m^{-2} between 70 and 80°N in each of the three RCPs in EP. While the zonal change in mean annual SWE is highly dependent on RCPs during the MP and LP, particularly at higher latitudes. South of 60°N, the relative changes in SWE during the MP are similar for all three RCPs. However, between 70° and 80°N, the decrease in SWE is -36 kg m^{-2} for RCP2.6, -44 kg m^{-2} for RCP4.5, and -55 kg m^{-2} for RCP8.5. Moreover, the reduction in SWE is more pronounced in the LP than during the EP and MP, particularly for RCP8.5. We note that the maximum increase in temperature and decrease in SWE both occur at high latitudes, suggesting a potential relationship between decreasing SWE and increasing temperature for different RCPs.~~

~~Figure 4 (a, d, g) illustrates an intriguing pattern of zonal maximum SWE (ZMSWE) variability. Relative to RP, the ZMSWE exhibits a general decline for all RCPs over the course of the 21st century. However, the ZMSWE shows a similar pattern for the three RCPs during the EP and MP, while the amounts of decline become highly variable during the LP for the three RCPs. This pattern suggests that the change in ZMSWE depends not only on RCP but also on the different periods (e.g., EP, MP, LP). In contrast, a large reduction in ZMSWE occurs between 30° and 40°N for all three RCPs during the EP, MP and LP, and is potentially linked to the strong reduction in SWE over the TP (Figure 3).~~

~~As the only cold, high-altitude region in the mid-latitude NH, the unique topographic and cryospheric effects of the TP may have affected the performance of model simulations in this region. Nonetheless, we note the modeled output generally captured the main features of the observations (Figure 1).~~

~~We also note that a second, larger decline in ZMSWE occurs at 60–70°N during LP for RCP8.5, this change always accompanies with the amplified warming at the high latitudes, and the magnitude of this decline in SWE is greater than that at 30–40°N. But this result disagrees with the findings of Brutel-Vuilmet et al (2008), who suggested that the relative reduction in ZMSWE would be greatest at lower altitudes (20–30°N). According to that study, the low-latitude decline in ZMSWE is driven by strong snowfall reduction, and the changes are weak farther north despite the stronger warming (Brutel-Vuilmet et al., 2008). Other studies also argue that the most significant decrease in ZMSWE occurs at low elevation in mountainous regions (e.g., Maloney et al., 2012); however, the present results In this study show that the significant change in ZMSWE may also occur at higher elevations (e.g., the TP).~~

~~As shown in Figure 4 g, the magnitude of the decrease in ZMSWE during the LP for RCP8.5 is greater than for the two lower-emissions pathways (RCP2.6 and RCP4.5), particularly at higher latitude. This pattern also indicates a role for temperature in driving changes in ZMSWE, with the exception of the influence of elevation.~~

The above results show that both the relative and absolute changes in SWE show a tendency to decline with time and with increased emissions. The most significant relative reduction in SWE occurs at low latitudes, where snow may gradually disappear with the temperature increasing in the 21st century. Another significant relative and absolute change in SWE occurs in the Arctic, where significant temperature and precipitation increases are projected. This result indicates that decreasing SWE will likely lead to acceleration of the hydrologic cycle.

In general, precipitation increases will lead to an increase in SWE, however, at high latitudes SWE does not increase alongside increased precipitation in all RCPs and periods (Figure 4), which indicates that the decrease in SWE is governed by temperature. However, the Arctic (north of 70°N) is characterized by significant increases in temperature and precipitation, and a significant decrease in SWE. This result suggests that the fraction of accumulated snowfall that remains on the ground (snow cover) will decrease, and it reflects the non-linear relationships between temperature and precipitation and accumulated snowfall.

To analyze the relationships between the decrease in SWE and the increase in temperature, Table 2 shows slopes of the regression between projected interannual SWE and temperature, and the correlation coefficients for SWE and temperature at different latitude bands in the three RCPs. During the EP, linear relationships between SWE and temperature are significant in all latitude bands, which illustrates that SWE decreases alongside increasing temperature. There are also significant negative correlations between SWE and temperature; i.e., increasing temperature leads to decreasing SWE. However, for RCP2.6 this relationship is only observed in the EP, and not in the MP and LP except in the 40–50°N latitude band. Similarly, for RCP4.5 there is significant negative relationship between SWE and temperature in the EP. This relationship is observed north of 40°N in the MP, and gradually moves northward, only occurring in the 40–60°N latitude band in the LP. Of note, a significant negative relationship between SWE and temperature is observed in RCP8.5 during all three periods.

A comparison of Figure 4 with Table 2 shows that although temperature is a key factor in controlling SWE, the rate of the temperature increase is not the same as the rate of the SWE decrease. In other words, SWE decreases in response to a specific temperatures range.

~~According to AR5 (Stocker et al., 2013), anthropogenic warming will be~~

~~most pronounced at high latitude, and the temperature increase further leads to changes in water exchange and the water cycle. Additionally, such enhanced warming will influence the rainfall-to-snowfall ratio of winter precipitation, potentially driving changes in snow cover and/or SWE. Table 2 shows projected changes in the zonal relationship between mean annual SWE and temperature. Relative to RP, the rate of decline in mid-latitude SWE will increase with rising temperature for the mid–low emissions pathways. In contrast, the sensitivity of SWE to temperature gradually decreases from the EP to the LP for RCP8.5, suggesting the rate of reduction in SWE might decline as temperature increases beyond a certain level.~~

In AR4 (~~Meehl et al~~IPCC. 2007), temperatures in the 40−60°N latitude band were closely correlated with the area of springtime snow cover (r =-0.68). This correlation increased to -0.76 in AR5 (~~Stocker et al.~~IPCC, 2013). The present results support those findings, suggesting that the most significant changes in SWE will occur at mid to high latitudes during winter and spring (not shown). Furthermore, the correlation between SWE and temperature during different periods of 21st century is stronger, even more than that reported by AR5 (~~Stocker et al.~~IPCC, 2013), indicating that SWE at mid to high latitudes will persistently decrease with the rising temperature.

带格式的: 上标

4.2 Seasonal changes in SWE

Figure 5 depicts ~~seasonal~~ monthly changes in ~~monthly~~ SWE and its relative change (RE) ~~averaged~~ over ~~the~~ NH land~~masses~~ (excluding Greenland) during different periods of the 21st century.~~the RP, EP, MP and LP. The~~ M~~m~~ulti-model ensemble simulations during the RP ~~shows that simulations during the RP are consistent with the observed SWE, reproducing~~ reproduce the basic features of monthly variation in observed SWE (GlobSnoe), with the maximum values ~~during~~ in spring, and minimum ~~values~~ SWE ~~during~~ in summer (not shown). These same features are evident in simulations of the EP, MP, and LP for the three different RCPs (Figure 5a-c), although the main difference ~~being~~ is that total SWE throughout the 21st century is lower than during the RP.

~~amounts are lower than those during the RP. Figure 5 (b, d, f) shows changes in SWE during the EP, MP and LP for all three RCPs, relative to RP. For all three periods of the 21st century, the greatest decrease in SWE occurs during spring, while the smallest reduction occurs in summer, contrary to the pattern of monthly SWE change. The magnitude of the decrease in SWE is similar for each RCP during the EP (Figure 5 b), that is, in the first 20 years of 21st century, the change in SWE relative to RP is the same in all three RCPs, but differences among the RCPs are evident during the MP and LP (Figure 5 d, f). During the LP, the maximum decline reaches -26.39 kg m^{-2} for RCP8.5, while the values range from -13.85 to -17.45 kg m^{-2} for RCP2.6 and RCP4.5, respectively. RCP has stronger effects on SWE change in LP than in EP and MP, although the model uncertainty caused by integration cumulative errors is enlarged from EP to LP. However, the simulation still basically reproduces the features of SWE. Thus, regardless of RCP or time period, the reduction in SWE during the winter half-year exceeds that in the summer half-year, in keeping with the results shown in Figure 3.~~

Figure 5d–f shows changes (RE) in SWE during the EP, MP and LP for all three RCPs relative to the RP. For all three periods of the 21st century, the greatest decrease in SWE occurs during summer, while the smallest reduction occurs in spring. In the first 20 years of the 21st century, the change in SWE relative to the RP is the same in all three RCPs (Figure 5d), and differences among the RCPs are more evident during the MP and LP (Figure 5e–f). During the last period of the 21st century (LP), the maximum reduction in SWE is 66.4% for RCP8.5, and ranges from 27.5% for RCP2.6 to 39.8% for RCP4.5. In contrast, the largest absolute change in SWE appears in spring, with the smallest decline in summer. The relative change in SWE is thus predicted to be markedly different to the absolute change.

~~As the dominant parameters influencing SWE, t~~Temperature and precipitation are the dominant parameters influencing SWE, and both exhibit considerable changes in seasonality (Figure 6). Relative to the RP, temperatures are projected to rise during the EP (Figure 6a), MP (Figure 6c) and LP (Figure 6e) for all three RCPs, with the greatest warming occurring in winter and the smallest in summer. The magnitude of the temperature change increases with higher emissions over time. In the EP, the temperature increase does not exceed 2°C for all three RCPs, and larger differences emerge during the MP and LP. Moreover, a basic feature is that the temperature increase is significant in the tropics and Arctic regions during the three periods of 21st century.~~both exhibit considerable changes in seasonality (Figure 6). Relative to RP, temperatures for all three RCPs are projected to rise during the EP (Figure 6 a), MP (Figure 6 c), and LP (Figure 6 e), with the greatest warming occurring in winter, and the smallest in summer. Similar results in EP (Figure 6 a) show that the temperature increase does not exceed 2°C, which is consistent with the results in AR5. During later periods, the magnitude of warming varies according to RCP, particularly during the LP, for which the RCP8.5 simulation produces a larger change than the other two emissions pathways (Figure 6 e).~~

Precipitation also increases throughout the 21st century for all three RCPs (Figure 6d–f), and changes in precipitation during winter exceed those during summer, despite the larger absolute change in precipitation in summer. During the EP, the magnitude of precipitation increase is the same for all three RCPs, and the change gradually grows larger with increased emissions over time. A noticeable feature of the model outputs is that changes in precipitation for mid–low emissions are not significant during the MP and LP, the largest increase in precipitation occurs during winter in the LP for RCP8.5, and the RE exceeds 20%.

~~Precipitation also exhibits an increasing trend for the different RCPs, with the smallest increase occurring in spring, coincident with the largest decrease in SWE during spring. Simulated changes in precipitation are similar for the different RCPs during the EP (Figure 6 b), but diverge during the MP (Figure 6~~

~~d) and LP (Figure 6 f), indicating that the magnitude of projected precipitation changes is dependent on RCP and the time period. The most significant increase in precipitation occurs during the LP for RCP8.5. While the rise in temperature during the winter half-year is larger than that of the summer half-year, the opposite is true for precipitation, with the greatest increase taking place during the summer half-year. This pattern implies that decreasing SWE is attributable to increasing temperature and the minor increase in precipitation~~

SWE tends to decrease alongside the increase in global temperature throughout the 21st century. To further validate this finding for SWE in different RCPs, Table 2 shows the regression slope for mean annual SWE and mean temperature over different latitude bands in the NH during the RP, EP, MP and LP. The results show a significant decrease in SWE for RCP8.5 during the EP, MP and LP. However, for the mid–low emission scenario, a significant decrease in SWE at different latitude bands only occurs persistently in the EP. In the MP and LP, a significant decrease in SWE occurs mainly in the mid–high latitude band. The distribution in the linear trend of mean annual SWE (not shown) shows decreases over northern North America and the TP, and increases over Siberia. This pattern indicates that the change in mean annual SWE is spatially variable, which is consistent with the spatial change shown in Figure 3.

带格式的: 缩进: 首行缩进: 1.5 字符

~~To differentiate between the relative contributions of temperature and precipitation to SWE, we calculated partial correlations between the SWE and temperature and precipitation. Table 3 shows that for each time period of the 21st century, SWE has a strong negative partial correlation with temperature and weak correlation with precipitation. The significantly negative partial correlation for RCP8.5 decreases from EP to LP in the winter half-year, implying that the rate of decline should diminish as a consequence of rising temperature. We also note that the partial correlation between SWE and temperature during the spring uniformly passes the 90% significance test~~

~~during the EP, MP, and LP for RCP8.5, resulting in a persistent decline in springtime SWE. The largest decline in simulated SWE also occurs in spring, consistent with the results shown in Figures 3 and 5, the decrease in SWE is related to the increasing temperature. Räisänen (2008) proposed that changes in snow conditions will most likely depend on present-day temperature, in close agreement with our results.~~

~~The correlation between SWE and temperature in Table 2 reflects the relation of SWE decreasing to the increasing temperature. The sensitivity of SWE to temperature shows a gradually increase over the 21st century form the south to the north. The correlation is significant in most latitude zones (north of 30°N) in EP, but not in MP or LP, in all three RCPs, and is only significant north of 30°N under RCP8.5 in the EP, MP and LP. In addition, SWE is only weakly related to temperature in MP and LP except for several latitude zones in RCP2.6, suggesting that the temperature increase is not always linked to a decreasing SWE.~~

~~4.3 Trend changes in SWE~~

~~To further analyze the SWE changes in different RCPs, Figure 7 shows the annual and seasonal SWE trend distribution during 2006–2099 in the NH. The results show that the projected significant changes in SWE occur at mid to high latitudes, with a decreasing trend over the northern North America and the TP, and an increasing trend over Siberia. This pattern shows that the rate of SWE change is spatially variable. The CMIP5 multi-model ensemble projects a decreasing trend in SWE in most regions over the NH landmasses between 2006 and 2099 (Figure 7). For RCP2.6, the mean annual SWE is projected to decrease considerably over the TP, where the annual mean trend is less than -4 kg m^{-2}/10a, which is consistent with the temperature increasing rapidly at high elevations in mid-latitude regions. Coastal Alaska is another region where SWE changes are evident, and the trend here is between -1.5 and -1 kg m^{-2}/10a. In other regions, trends range from -0.5 to 0.5 kg m^{-2}/10a for RCP2.6. An increasing trend is projected for central Asia and eastern~~

~~Siberia.~~

~~For RCP4.5, the areal extent of the significant reduction in SWE increases over both the TP and coastal Alaska, and the notably decreasing trend over the TP reflects the decreasing SWE in response to increasing temperature, with the exception of the influence of terrain. For RCP8.5, the mean annual SWE is projected to decline over North America, particularly in western North America and eastern Canada, where the trend is smaller than -4 kg m^{-2}/10a. In the Eurasia region north of 45°N, SWE is projected to increase in the east (eastern Siberia) and decrease in the west. Another significant negative trend is located over central Russia, where the negative trend in SWE ranges from -3.5 to -3 kg m^{-2}/10a. At mid-low latitudes in Eurasia, the most significant reductions in mean annual SWE still occur over the TP. Compared with the lower-emissions pathways (RCP2.6, RCP4.5), the magnitude of decline or increase in SWE is greater for RCP8.5. Specifically, the CMIP3 models show that mean annual SWE will increase over eastern regions and decrease over western regions of Eurasia between 2003 and 2060, and that the intensity of SWE changes is greater under higher-emissions scenarios (e.g., A2) than under lower-emissions scenarios (e.g., B1) (Ma et al., 2011).~~

On~~At~~ a~~the~~ seasonal scale, ~~projected trends in SWE over the NH landmasses are weaker during the summer half-year than the winter half-year for all three RCPs. During winter, in Eurasian north of 45°N, SWE exhibits an increasing trend in the east and a decreasing trend in the west. In contrast, trends in wintertime SWE are uniformly negative over North America and the TP. From the lower emissions to the higher emissions, both the increasing and decreasing trends become more pronounced. In contrast,~~ the extent and ~~intensity~~ magnitude of the SWE increase~~mental SWE~~ in winter is larger than ~~that~~ in spring, but the ~~reduction~~ range and ~~strength~~ magnitude of SWE decrease is significantly smaller than ~~that~~ in spring. This is due to the later shift from liquid to solid precipitation in autumn and an earlier onset of snowmelt in

带格式的: 缩进: 首行缩进: 1.5 字符

spring (Räisänen, 2008). Consequently, the reduction in SWE averaged over the NH is more significant in spring than in winter.~~; consequently, the absolute scale of reduction in SWE is larger in spring than in winter.~~

~~Although ensemble simulations show that SWE decreases throughout much of the NH during the three RCPs investigated, we note that there remains a significant increasing trend in SWE across Siberia in winter and spring. Nonetheless, owing to the greater geographical extent and magnitude of the projected reductions, the average trend for the NH in the 21st century is for progressively declining SWE.~~

There is high model uncertainty of SWE simulation in the 21st century, especially for RCP8.5, this is illustrated in Figure 7, which also shows the range of uncertainty in the mid–low emission scenario. However, despite model uncertainty, ~~The projected changes in mean annual SWE over NH landmasses in the three RCPs are shown in Figure 8 and Table 4. Relative to RP, mean~~ annual SWE still ~~-~~exhibits a consistent and significant decline for each of the three RCPs, with linear trends of −0.54 kg m^{-2}/10a for RCP2.6, −1.09 kg m^{-2}/10a for RCP4.5 and −2.05 kg m^{-2}/10a for RCP8.5 ~~-0.54, -1.09, and -2.05 kg m^{-2}/10a for RCP2.6, RCP4.5, and RCP8.5~~ (Table 3~~4~~).~~,~~ ~~respectively. After 2040,~~ Figure 7 also shows that the negative trend in SWE gradually begins to level out for RCP2.6, and weakens somewhat for RCP4.5. For RCP8.5, however, the SWE continues to decline beyond the end of the 21st century, which agrees with projections of snow cover extent (Zhu and Dong, 2013).~~consistent with anticipated reductions in snow cover (Brutel et al., 2012).~~

Despite the fact that ensemble simulations show decreasing SWE throughout much of the NH during the three RCPs investigated, we note a significant increasing trend in SWE across Siberia in winter and spring. Nonetheless, owing to the greater geographical extent and magnitude of the projected reductions, there is an overall negative trend in NH SWE during the 21st century.

带格式的: 缩进: 首行缩进: 1.77 字符

5 Contribution analysis for SWE change~~Changes in SWE with rising temperature~~

In both seasonal and zonal contexts, rising temperatures play a fundamental role in projected SWE. Figure 6 shows that the most significant increases in temperature and precipitation occur in winter, but the largest reduction in SWE appears in summer. To ~~analyze~~ identify the relative contributions ~~impact~~ of temperature and precipitation to changes in ~~on~~ SWE ~~in the 21st century~~, we calculate the partial correlation between SWE and temperature as well as between SWE and precipitation during the RP, EP, MP and LP for three RCPs (Table 4). SWE has a strong negative partial correlation with temperature and weak correlation with precipitation throughout the 21^{st} century. The negative partial correlation for RCP8.5 decreases from the EP to the LP in the winter half-year, indicating that the rate of the SWE decrease should decline as temperature increases. We also note that the partial correlation between SWE and temperature during the spring uniformly passes the 90% significance test during the EP, MP and LP for RCP8.5, resulting in a persistent decline in springtime SWE, despite the increase in precipitation.~~the ratios of SWE decrease to temperature increase are calculated for the three RCPs during the EP, MP, and LP (Figure 9). The ratios reflect the sensitivity of SWE to temperature. Similar linear relations have been reported for sea ice (Mahlstein and Knutti, 2012) and permafrost (Slater, 2013), indicating that increasing temperature plays a central role in cryospheric change. As shown in Figure 9, the slopes for EP, MP, and LP (-1.47 to -2.50 kg m⁻²°C⁻¹) are less than that for the RP (-3.17 kg m⁻²°C⁻¹), implying that the rate of decrease in SWE ultimately will decline with persistent~~

带格式的：定义网格后不调整右缩进，行距：2 倍行距，不对齐到网格

~~temperature rise. Furthermore, we note that the sensitivity of SWE to temperature increases gradually from the EP to LP for a single emissions pathway, and over the same period the sensitivity decreases when moving from the lower-emissions to higher-emissions pathways. Thus, the impact of temperature on SWE is dependent on the magnitude and duration of emissions forcing.~~

Relative to 1986–2005, the largest absolute decline in simulated SWE also occurs in spring, indicating that the decrease in SWE is related to earlier temperature-driven snowmelt. This result agrees with Räisänen (2008) who proposed that changes in snow conditions would likely depend on present-day temperature. With the increasing temperature, the sensitivity of SWE to temperature averaged over the NH gradually increases from the EP to the LP for the same RCP (not shown).

Temperature increase may change the water cycle and rain–snow ratio (fraction of solid precipitation), and will act to increase the rate of snow melt (fraction of accumulated snowfall). Actually, as shown by Equation 4, SWE can be affected by changes in total precipitation, the fraction of precipitation that falls as snow and the fraction of accumulated snowfall that has not melted. Räisänen (2008) used CMIP3 model simulations to analyze the contributions of the above factors to SWE in Finland and eastern Siberia, and suggested that the major contributor to the change in SWE varies regionally. Thus, over the whole NH, how about the effect of total precipitation, snowfall and accumulated snowfall on SWE during the different periods of the 21st century.

~~Furthermore, a linear relationship between SWE and temperature is found for all three RCPs and all three periods (Table 2). The linear regression slope reflects the response of SWE to the increasing temperature. The sensitivity of SWE to temperature gradually declines over the course of the~~

~~21st century for RCP8.5, suggesting a threshold for the relationship between SWE and temperature. That is, if the temperature increases to a certain level, the rate of decline in SWE will slow down.~~

Figure 8 shows the contributions of total precipitation, snowfall and accumulated snowfall to the changes in SWE for three RCPs during three periods of 21st century. During the EP, total precipitation shows an increase in all months, but snowfall decreases in all months. This indicates that changes in total precipitation and snowfall have competing effects and lead to an increase and decrease in SWE, respectively. Because the magnitude of the decrease in snowfall is larger than the increase in total precipitation, the reduction in SWE is attributed to changes in the fraction of precipitation that falls as snow. The contributions of total precipitation, snowfall and accumulated snowfall grow larger with time. During the LP, temperature increases cause the change in accumulated snowfall to be larger than the change in snowfall after May, so that the former becomes the main control on SWE. In general, from August to May in the next year, the change in SWE is generally related to changes in snowfall, but after May increased melting efficiency dominates the change in SWE.

6 Summary and conclusions

We employed ~~twenty~~ 20 CMIP5 climate models to investigate projected changes in SWE for the 21st century~~, using~~ under three different RCPs. ~~We find that, relative to RP, mean annual SWE for all three RCPs exhibits a~~The results show a decrease in mean annual SWE for all three RCPs ~~negative trend~~ over much of the NH landmasses relative to the RP. The most significant reductions occur over the TP and ~~the majority of~~ North America, while a minor increase occurs over Siberia, however, the overall pattern in the NH is one of declining SWE. ~~.~~Moreover, we suggested that the intensity of changes in SWE is greater for RCP8.5 than for RCP4.5 and RCP2.6, and that these changes are most pronounced at mid to high latitudes. Since both the magnitude and geographic extent of the changes are much greater in spring than in winter, the overall pattern in the NH is one of declining SWE, with the most significant losses occurring in spring. The multi-model ensemble suggests that the negative trend in SWE ~~for RCP2.6 will~~ begins to level out or become stable for RCP2.6 and weakens somewhat for RCP4.5, ~~diminish after 2040,~~ whereas the declining trend continues beyond the end of the 21st century for RCP8.5. The patterns of change in SWE in spring and winter are the same with the mean annual SWE, since both the magnitude and geographic extent of the reduction in SWE are much greater in spring than in winter, the significant reduction in SWE over NH occurs in spring, however, the largest percent change in SWE does not occur in spring, but in summer, and this indicates that the change in SWE is related to baseline SWE.

带格式的：非突出显示

Changes in SWE are accompanied by increasing temperature and precipitation during the winter half-year~~, most notably in spring~~. SWE is not simply a function of temperature, ~~However,~~ but the partial correlations between SWE and both temperature and precipitation indicate that ~~considerable~~ decreases in SWE can be attributed primarily to increasing temperatures. Furthermore, we note that while atmospheric warming occurs primarily ~~preferentially~~ during the winter half-year, coincident with the ~~small~~ greater increase ~~projected increase~~ in precipitation, ~~but the increase~~ greater precipitation cannot compensate for the increased snowmelt due to rising temperatures.

Projections of mean annual SWE exhibit a declining trend~~s~~ and the magnitude of the SWE relative decrease is gradually reduced from south to north over NH. Namely, a more significant reduction in mean annual SWE for all three RCPs occurs at low latitudes throughout the 21st century, accompanied by an anticipated warming trend. Annual maximum SWE also has similar features to mean annual SWE, with the largest decrease observed at low latitudes. However, ~~with increasing latitude. Specifically, a more significant reduction in mean annual SWE for all three RCPs occurs between~~

~~70° and 80°N for the three time periods of the 21st century, accompanied by an anticipated warming trend. Moreover, ~~the correlation between mean annual SWE and temperature ~~is significant at high latitudes, and the data ~~suggests that a threshold of the relationship between the SWE and temperature would ~~restrain ~~mitigate the persistent ~~decline ~~decrease in SWE with increasing temperature. ~~For ZMSWE, the results also show a larger-scale decrease in ZMSWE centered between 30° and 40°N for all RCPs during the three periods investigated, which reflects the influence of terrain on SWE; and other pronounced reduction occurs at high latitude during the LP, only for RCP8.5, implying that, with the exception of topography, changes in ZMSWE are influenced primarily by temperature.~~

The 21st century temperature increases are projected to have a pronounced effect on rain–snow ratios and snowmelt. Precipitation also shows an increasing trend, however, because the magnitude of the reduction in snowfall is larger than the increase in total precipitation, the decreasing snowfall becomes the major contributor to the reduction in SWE from August to May in the next year during the 21st century. As the temperature increase, efficient snowmelt dominates the change in SWE after May, especially during the LP. ~~An intriguing feature of the modeled projections is that, although decreasing SWE invariably accompanies the increasing temperature, ratios of SWE decrease to temperature increase are highly variable among the RCPs and modeled time periods. The results suggest that this pattern reflects diminished sensitivity of SWE to temperature during the EP, MP, and LP relative to the RP. As mean annual temperature increases, the rate of decline in SWE will decrease, a pattern that is dependent not only on the specific RCP but also on the integration time period (e.g., EP, MP, LP). ~~Finally, aAlthough ~~the ~~model projection have increasing ~~results contain ~~uncertainty later in the 21st century, the trends observed in the simulations remain consistent,~~ies due to errors caused by integration truncation and inter-model differences,~~ and increased model error and bias do not appear to~~this does not~~ affect the

带格式的: 缩进: 首行缩进: 1.5 字符

带格式的: 上标

~~generality or the value of the main~~ conclusions of this study.

Author contributions. C. H. Wang contributed to the idea and conception of this study, analysis of the result and arrangement the framework of the manuscript.

H. X. Shi carried out the analysis of the data and writing the manuscript with the assistance of C. H. Wang.

Acknowledgments. This work was supported by the National Natural Science Foundation of China (2013CBA01808, 91437217, 41275061). The snow water equivalent data used in this study are from European Space Agency (ESA) GlobSnow product and CMIP5 model outputs.

References

Brown, R. D., and Mote, P. W. : The response of Northern Hemisphere snow cover to a changing climate. Journal of Climate, 22, 2124-2145, 2009.

~~Barnett, T. P., Adam, J. C. and Lettenmaier D. P. : Potential impacts of a warming climate on water availability in snow-dominated regions. Nature, 438, 303-309, doi:10.1038/nature04141, 2005.~~

Brutel-Vuilmet, C., Ménégoz, and Krinner, G. : An analysis of present and future seasonal Northern Hemisphere land snow cover simulated by CMIP5 coupled climate models. The Cryosphere, 7, 67-80, doi:10.5194/tc-7-67-2013, 2013.

~~Bulygina, O. N., Razuvaev V. N. and Korshunova , N. N. : Changes in snow cover over Northern Eurasia in the last few decades. Environmental Research Letters, 4, 045026, doi:10.1088/1748-9326/4/4/045026, 2009.~~

Chen, S. B., Liu, Y. F., Thomas A. Climatic change on the Tibetan Plateau: potential evapotranspiration trends from 1961－2000[J]. Climatic Change, 76, 291-319, 2006.

带格式的：字体：非加粗

~~Clark, M. P., Serreze, M. C. and McCabe, G. J. : Historical effects of El Nino and La Nina events on the seasonal evolution of the montane snowpack in the Columbia and Colorado River Basins. Water Resources Research, 37, 741-757, doi.1029/2000WR900305, 2010.~~

Falarz, M. : Long-term variability in reconstructed and observed snow cover over the last 100 winter seasons in Cracow and Zakopane (South Poland). Climate Research, 19, 247-256, 2002.

Groisman, P. Y., Knight, R. W., Karl, T. R., Easterling, D. R., Sun, B., and Lawrimore, J. H.: Contemporary changes of the hydrological cycle over the contiguous United States: Trends derived from in situ observations. Journal of Hydrometeorology, 5, 64-85, 2004.

Hancock, S.; Baxter, R.; Evans, J.; Huntley, B. Evaluating global snow water equivalent products for testing land surface models. Remote Sens. Environ, 128, 107–117, 2013.

Hayhoe, K., Cayan, D., Field, C. B., Frumhoff, P. C., Maurer, E. P., Miller, N. L. and Verville, J. H.: Emissions pathways, climate change, and impacts on California. Proceedings of the National Academy of Sciences of the United States of America, 101, 12422-12427, 2004.

Hosaka, M., Nohara, D. and Kitoh, A.: Changes in snow coverage and snow water equivalent due to global warming simulated by a 20 km-mesh global atmospheric model. SOLA, 1, 93-96, doi: 10.2151, 2005.

~~Houghton, J. T., Ding, Y., Griggs, D. J., Noguer, M., vander Linden, P.J., Dai, X., Maskell, K. and Johnson, C. A. : Summary for Policymakers. In : Climate change 2001: The Scientific Basis. Contribution of working Group I to the Third Assessment Report of the Intergovernmental Panel on Climate Change. Cambridge University Press, Cambridge, United Kingdom and New York, NY, USA, pp,4, 2001.~~

Ji, Z. M. and Kang, S. C.: Projection of snow cover changes over China under RCPs scenarios. Climate dynamics, 41, 589-600, 2012.

Lemke, P., Ren, J., Alley, R. B., et al. Observations: changes in snow, ice and frozen ground[J]. Titel: Climate change 2007: the physical science basis; summary for policymakers, technical summary and frequently asked questions. Part of the Working Group I contribution to the Fourth Assessment Report of the Intergovernmental Panel on Climate Change, 2007: 337-383.

Liu, X. X, Chen, B, D. Climatic warming in the Tibetan Plateau during recent decades[J]. International journal of climatology, 20: 1729-1742, 2000.

Maloney, E. D., Camargo, S. J., Chang, E., et al. North American Climate in CMIP5 Experiments: Part III: Assessment of 21st Century Projections[J]. Journal of Climate. 2014, 27: 2230-2270.

~~Ma, L. J., Luo, Y. and Qin, D. H.: Snow Water Equivalent over Eurasia in Next50YearsProjected by CMIP3Models. Journal of glaciology and geocryology, 33, 707-720, 2011.~~

~~Mahlstein, I. and Knutti, R. : September Arctic sea ice predicted to disappear near 2℃ global warming above present. Journal of Geophysical Research, 117, D06104, doi:10.1029/2011JD016709, 2012.~~

~~McCabe, G. J. and Dettinger, M. D. : Primary modes and predictability of year-to-year snowpack variations in the western United States from teleconnections with Pacific Ocean climate. Journal of Hydrometeorology, 3, 13-25, 2002.~~

带格式的: 缩进: 悬挂缩进: 1.59 字符, 左 -0.23 字符, 首行缩进: -1.59 字符, 行距: 固定值 20 磅

Meehl, G. A., Stocker, T. F., Collins, W. D., Friedlingstein, P., Gaye, A.T., Gregory, J. M., Kitoh, A., Knutti, R., Murphy, J. M., Noda, A., Raper, S. C. B., Watterson, I. G., Weaver, A. J., and Zhao, Z. C. : Global Climate Projections. In: Climate Change 2007: The Physical Science Basis. Contribution of Working Group I to the Fourth Assessment Report of the Intergovernmental Panel on Climate Change [Solomon, S.,D. Qin, M. Manning, Z. Chen, M. Marquis, K.B. Averyt, M. Tignor and H.L. Miller (eds.)]. Cambridge University Press, Cambridge, United Kingdom and New York, NY, USA, pp, 772, 2007.

Mote, P. W.: Climate-Driven Variability and Trends in Mountain Snowpack in Western North America. Journal of Climate, 19, 6209-6220, 2006.

Mote, P. W., Hamlet, A. F., Clark, M. P. and Lettenmaier, D. P. : Declining mountain snowpack in western North America. Bulletin of the American Meteorological Society, 86, 39-49.

Pierce, D. W., et al. Attribution of declining Western U.S. snowpack to human effects[J]. Journal of Climate. 21, 6425–6444, 2008.

~~Pulliainen, J., J. Grandell, and M. T. Hallikainen. HUT Snow Emission Model and its Applicability to Snow Water Equivalent Retrieval. IEEE Transactions on Geoscience and Remote Sensing. 37: 1378-1390, 2006.~~

Räisänen, J. : Warmer climate: less or more snow? Climate Dynamics, 30, 307-319, 2008.

Räisänen, J. and Eklund, J. : 21st Century changes in snow climate in Northern Europe: a high-resolution view from ENSEMBLES regional climate models. Climate Dynamics, 38 : 2575–2591, doi:10.1007/s00382-011-1076-3, 2011.

~~Rawlins, M. A., Willmott, C. J., Shiklomanov, A., Linder, E., Frolking, S., Lammers, R. B., Vorosmarty, C. J. : Evaluation of trends in derived snowfall and rainfall across Eurasia and linkages with discharge to the Arctic Ocean. Geophysical Research Letters, 33, L07403, doi:10.1029/2005GL025231, 2006.~~

Scherrer, S. C., Appenzeller, C. and Laternser, M. : Trends in Swiss alpine snow days—the role of local and large scale climate variability. Geophysical Research Letters, 31, L13215, doi:10.1029/2004GL020255, 2004.

带格式的: 缩进: 左侧: 0 厘米, 悬挂缩进: 1.68 字符, 首行缩进: -1.68 字符

~~Slater, A. G. and lawrence, D. M. : Diagnosing Present and Future Permafrost from Climate Models. Journal of Climate, 26, 5608-5623, 2013.~~

Stewart, I. T., Cayan, D. R. and Dettinger, M. D. : Changes towards earlier streamflow timing across western North American. Journal of climate, 18, 1136-1155, 2005.

Stocker, T. F., Qin, D. H., Plattner, G. K., Tignor, M., Allen, S. K., Boschung, J., Nauels, A., Xia, Y., Bex, V., and Midgle, P. M. : Summary for Policymakers. In: Climate change 2013: The Physical Scientific Basis. Contribution of Working Group I to the Fifth Assessment Report of the Intergovernmental Panel on Climate Change. Cambridge University Press, Cambridge, United Kingdom and New York, NY, USA, pp, 4, 2013.

Takala, M.; Luojus, K.; Pulliainen, J.; Derksen, C.; Lemmetyinen, J.; Kärnä, J.P.; Koskinen, J.; Bojkov, B. Estimating northern hemisphere snow water equivalent for climate research through assimilation of space-borne radiometer data and ground-based measurements. Remote Sens. Environ. 115, 3517–3529, 2011.

Vavrus, S. : The role of terrestrial snow cover in the climate system. Climate dynamics, 29, 73-88, 2007.

Vojtek, M., Faško, P. and Šťastný, P. : Some selected snow climate trends in Slovakia with respect to altitude. Acta Meteorologica Universitatis Comenianae, 32, 17-27, 2003.

Wang, C. H., Li, J. and Xu, X. G. University of Quasi-3-year period of temperature in last 50 years and change in next 20 year in China[J]. Plateau Meteorology, 31: 126-136, 2012.

Wang, Z. L. and Wang, C.H. : Predicting the snow water equivalent over China in the next 40 years based on climate models from IPCC AR4. Journal of glaciology and geocryology, 34:1273-1283, 2012.

Zhu, X. and Dong, W. J. : Evaluation and projection of Northern Hemisphere March-April snow cover area simulated by CMIP5 coupled climate models. Progressus Inquisitiones DE Mutatione Climatis, 9(3): 173-180, 2013.

Table. 1. Models used in this study.

Number	Model	Institution	Resolution
1	BCC-CSM1-1	Beijing Climate Center, China	2.8° ×2.8°
2	BCC-CSM1-1(m)	Beijing Climate Center, China	1.3° ×1.1°
3	CanESM2	Canadian Center for Climate Modeling and Analysis, Canada	2.8° ×2.8°
4	CCSM4	National Center for Atmospheric Research, USA	1.25° ×0.94°
5	CNRM-CM5	Centre National de Recherches Meteorologiques / Centre Europeen de Recherche et Formation Avancees en Calcul Scientifique	1.4° ×1.4°
6	CSIRO-Mk3-6-0	CSIRO Atmospheric Research, Australia	1.875° 1.875°
7	FGOALS-g2	Chinese Academy of Sciences	1.4° ×6°
8	FIO-ESM	The First Institute of Oceanography, SOA, China	2.8° ×2.8°
9	GFDL-ESM2G	Geophysical Fluid Dynamics Laboratory, USA	2.5° ×2.0°
10	GISS-E2-H	ASA Goddard Institute for Space Studies, USA	2.5° ×2.0°
11	GISS-E2-R	NASA Goddard Institute for Space Studies, USA	2.5° ×2.0°
12	HadCEM2-ES	Met Office Hadley Centre, UK	1.875° × 1.25°
13	MIROC5	Atmosphere and Ocean Research Institute, Japan	1.4° ×1.4°
14	MIROC-ESM-CHEM	Japan Agency for Marine-Earth Science and Technology, Atmosphere and Ocean Research Institute, Japan	2.8° ×2.8°
15	MIROC-ESM	Japan Agency for Marine-Earth Science and Technology, Atmosphere and Ocean Research Institute, Japan	2.8° ×2.8°
16	MPI-ESM-LR	Max Planck Institute for Meteorology, Germany	1.9° ×1.9°
17	MPI-ESM-MR	Max Planck Institute for Meteorology, Germany	1.875° × 1.875°
18	MRI-CGCM3	Meteorological Research Institute, Japan	1.1° ×1.1°
19	NorESM1-ME	Norwegian Climate Center, Norway	2.5° ×1.875°
20	NorESM1-M	Norwegian Climate Center, Norway	2.5° ×1.875°

Table. 2. Zonal slope (Slop) of the regression of mean annual SWE and temperature, and correlation coefficients (Cor.) ~~between~~ for mean annual SWE and ~~mean~~ temperature for three RCPs. RP, EP, MP, LP represent the periods 1986−2005, 2016−2035, 2046−2065, and 2080−2099, respectively.

		RCP2.6				RCP4.5			RCP8.5		
Lat(°N)		RP	EP	MP	LP	EP	MP	LP	EP	MP	LP
20-30	S	-0.43*	-0.22	-1.45	-0.36	-0.52*	-0.25	-0.08	-0.23*	-0.23*	-0.08
	C	-0.55*	-0.22	-0.42*	-0.14	-0.69*	-0.34	-0.03	-0.45*	-0.48*	-0.30
30-40	S	-2.15*	-4.38*	-0.74	-1.02	-3.39*	-0.85	-2.86	-3.14*	-1.64*	-0.81*
	C	-0.64*	-0.91*	-0.13	-0.13	-0.77*	-0.29	-0.25	-0.84*	-0.78*	-0.68*
40-50	S	-1.00*	-0.84	-1.60	-2.97*	-1.69*	-1.06*	-3.02*	-1.77*	-0.89*	-0.76*
	C	-0.62*	-0.44*	-0.39	-0.55*	-0.80*	-0.48*	-0.71*	-0.86*	-0.74*	-0.82*
50-60	S	-3.27*	-3.82*	-0.39	-2.68	-3.28*	-3.24*	-2.62*	-3.25*	-2.55*	-1.33*
	C	-0.71*	-0.64*	-0.08	-0.28	-0.75*	-0.65*	-0.57*	-0.80*	-0.78*	-0.67*
60-70	S	-2.87*	-2.57*	-2.84	-3.64	-3.67*	-5.10*	-3.71	-4.10*	-3.70*	-2.84*
	C	-0.66*	-0.47*	-0.32	-0.33	-0.74*	-0.76*	-0.35	-0.71*	-0.83*	-0.73*
70-80	S	-10.2*	-16.9*	-0.30	-2.40	-4.57*	-5.23*	-2.10	-8.31*	-6.16*	-4.62*
	C	-0.88*	-0.72*	-0.02	-0.35	-0.65*	-0.81*	-0.06	-0.84*	-0.91*	-0.88*

Note: * values~~indicate that the slope and correlation~~ exceed the 95% significance test.

Table. 3. Trends in SWE over Northern Hemisphere land during 2006−2099 derived from the three RCPs. All trends are significant at 95% confidence level (Mann–Kendall test).

Trend (kg m^{-2}/10a)	RCPs		
	RCP2.6	RCP4.5	RCP8.5
Autumn	-0.51	-1.17	-1.83
Winter	-0.54	-1.18	-2.18
Spring	-0.61	-1.32	-2.39
Summer	-0.50	-1.09	-1.79
Mean	-0.54	-1.09	-2.05

Table. 4~~3~~. Partial correlations between mean annual SWE and both temperature (T) and precipitation (P) over Northern Hemisphere land for three RCPs. RP, EP, MP, LP represent the periods 1986−2005, 2016−2035, 2046−2065, and 2080−2099, respectively.

		RCP2.6				RCP4.5			RCP8.5		
Month		RP	EP	MP	LP	EP	MP	LP	EP	MP	LP
Jan	T	-0.29	-0.59*	-0.25	-0.1	-0.54*	-0.44*	-0.52*	-0.45*	-0.38*	-0.31
	P	-0.13	-0.22	-0.05	-0.13	0.1	0	-0.14	0.05	-0.05	-0.05
Feb	T	-0.42*	-0.2	-0.1	-0.37*	-0.25	-0.76*	-0.38*	-0.51*	-0.39*	-0.28
	P	0.05	-0.17	-0.11	0.04	-0.11	0.18	0.09	0.02	-0.05	-0.11
Mar	T	-0.22*	-0.26	-0.24	-0.54*	-0.42*	-0.17	-0.56*	-0.4*	-0.4*	-0.4*
	P	-0.07	-0.03	-0.09	0.22	-0.05	-0.18	0.05	-0.02	-0.03	0.01
Apr	T	-0.38*	-0.31	-0.14	-0.38*	-0.37*	-0.49*	-0.51*	-0.49*	-0.38*	-0.38*
	P	-0.06	-0.1	0.02	-0.01	-0.09	0.09	0.09	0.11	-0.08	-0.05
May	T	-0.36*	-0.33	-0.31	-0.34	-0.31	-0.46*	-0.5*	-0.48*	-0.42*	-0.41*
	P	-0.07	-0.1	-0.38	-0.06	-0.2	0.07	0.09	0.1	-0.06	-0.01
Jun	T	-0.43*	-0.33	-0.57*	-0.07	-0.26	-0.46*	-0.08	-0.45*	-0.39*	-0.38*
	P	-0.07	-0.09	0.12	-0.06	-0.11	0.11	-0.27	-0.04	0.02	-0.05
Jul	T	-0.48*	-0.48*	0.27	-0.26	-0.56*	-0.54*	-0.51*	-0.04	-0.46*	-0.24
	P	-0.11	0	-0.2	-0.14	-0.08	-0.02	0.05	0.02	-0.09	-0.02
Aug	T	-0.33	-0.48*	-0.36*	-0.21	-0.48*	-0.38*	-0.29	-0.47*	-0.48*	-0.4*
	P	-0.07	-0.25	-0.06	-0.03	0	0	-0.02	-0.18	0	-0.06
Sep	T	-0.35	-0.44*	-0.39*	0.13	-0.3	-0.1	-0.59*	-0.27	-0.24	-0.34
	P	-0.05	-0.13	-0.01	-0.14	-0.17	-0.07	0.14	-0.07	-0.15	-0.04
Oct	T	-0.35	-0.53*	0.18	0.16	-0.47*	-0.21	-0.5*	-0.33	-0.28	-0.25
	P	-0.08	0	-0.09	-0.52	-0.03	0.06	0.07	-0.1	-0.06	-0.06
Nov	T	-0.43*	-0.36*	-0.07	0.01	-0.53*	-0.47*	-0.21	-0.29	-0.21	-0.33
	P	-0.05	-0.11	-0.09	-0.28	0.15	-0.05	-0.2	-0.03	-0.17	0
Dec	T	-0.25	-0.5*	-0.12	0.08	-0.27	-0.58*	-0.35	-0.34	-0.28	-0.28
	P	-0.12	-0.05	-0.01	-0.29	-0.16	-0.05	-0.19	-0.03	-0.05	0.04

Note: * ~~indicate that the partial correlation~~ values exceed~~s~~ the 95% significance test.

~~Table. 4. Trends of SWE during 2006–2099 derived from the three RCPs. Each trend is significant at 95% confidence.~~

~~Trend (kg m^{-2}/10a)~~	~~RCPs~~		
	~~**RCP2.6**~~	~~**RCP4.5**~~	~~**RCP8.5**~~
~~Autumn~~	~~-0.51~~	~~-1.17~~	~~-1.83~~
~~Winter~~	~~-0.54~~	~~-1.18~~	~~-2.18~~
~~Spring~~	~~-0.61~~	~~-1.32~~	~~-2.39~~
~~Summer~~	~~-0.50~~	~~-1.09~~	~~-1.79~~
~~Mean~~	~~-0.54~~	~~-1.09~~	~~-2.05~~

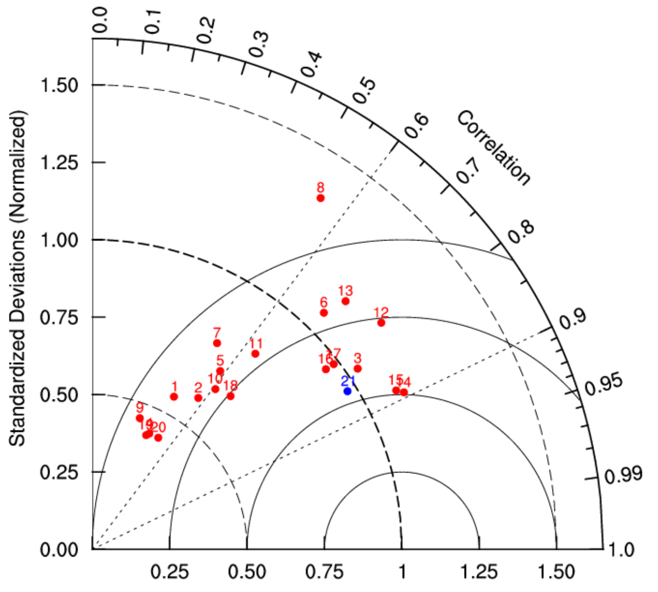

Figure. 1. Spatial correlation and standard variance ratios between observed and simulated (20 models) winter (DJF) mean SWE during 1980-2005. The numbers 1-20 ~~indicates the 20 models used in this paper, and~~ refer~~s~~ to the model names in Table 1.The number 21 indicates the multi-model ensemble. The vertical axis indicates the standard deviation ratios, and the numbers along the arc are the spatial correlation.

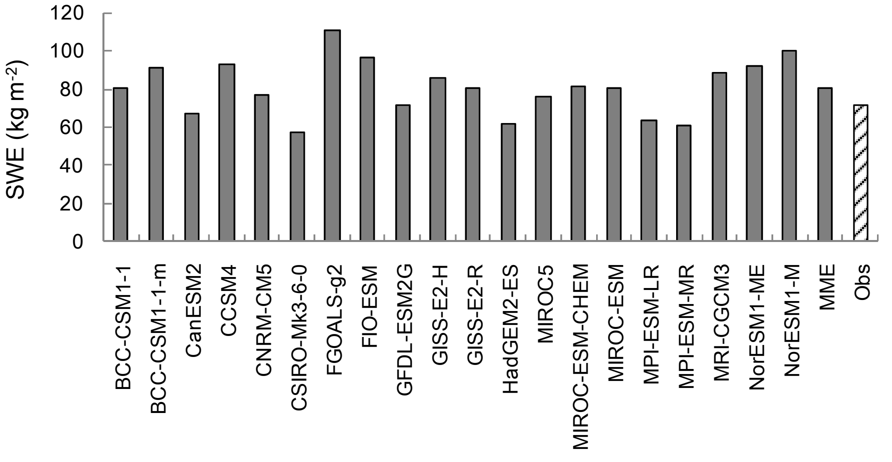

Figure. 2. The average of the observed and stimulated winter (DJF) mean SWE over the N~~n~~orthern Hemisphere land during 1980-2005. The multi-model ensemble (MME) refers to a combination of the 20 models listed in Figure 1. ~~(The 'MME' comprises the 20 preceding models listed in the figure).~~

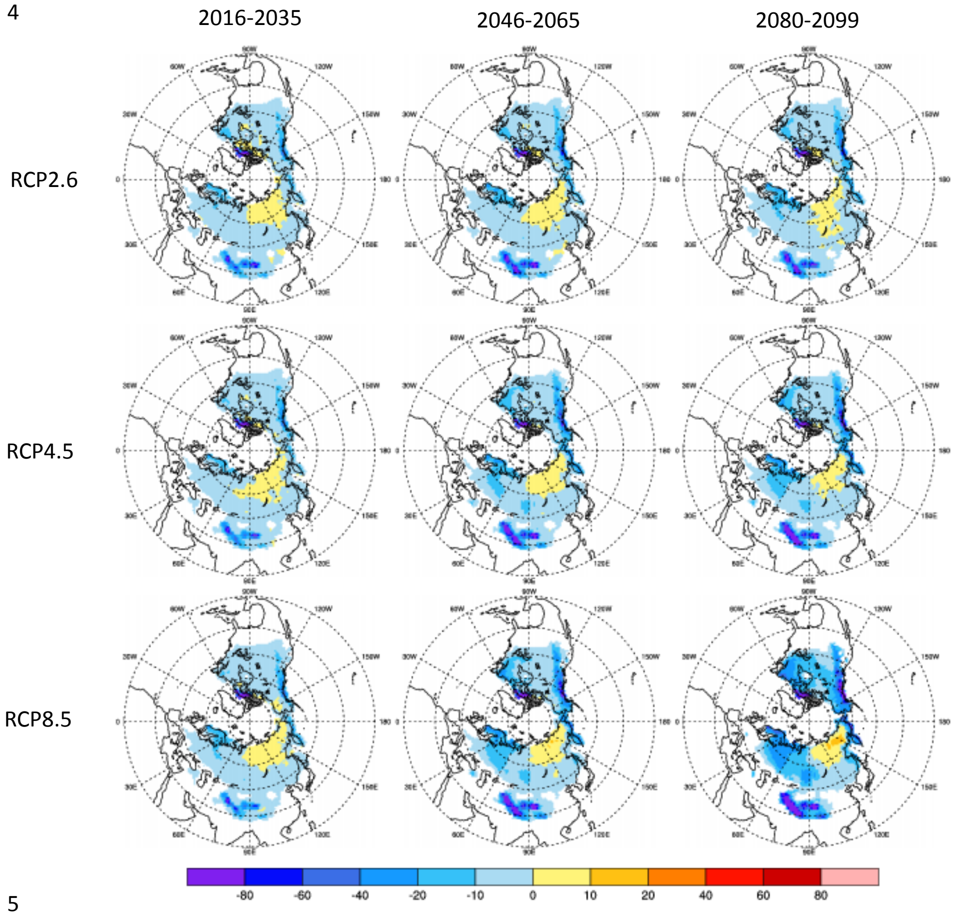

~~Figure. 3. Changes in mean annual SWE (kg m^{-2}) projected by the CMIP5 ensemble, relative to the period of 1986-2005. The three rows indicated the three scenarios RCP2.6, RCP4.5, and RCP8.5, respectively, the three columns are the three periods of 2016-2035, 2046-2065 and 2080-2099, respectively.~~

Figure. 3. Relative changes in mean annual SWE (%) projected by the CMIP5 ensemble, relative to the 1986−2005 reference period.

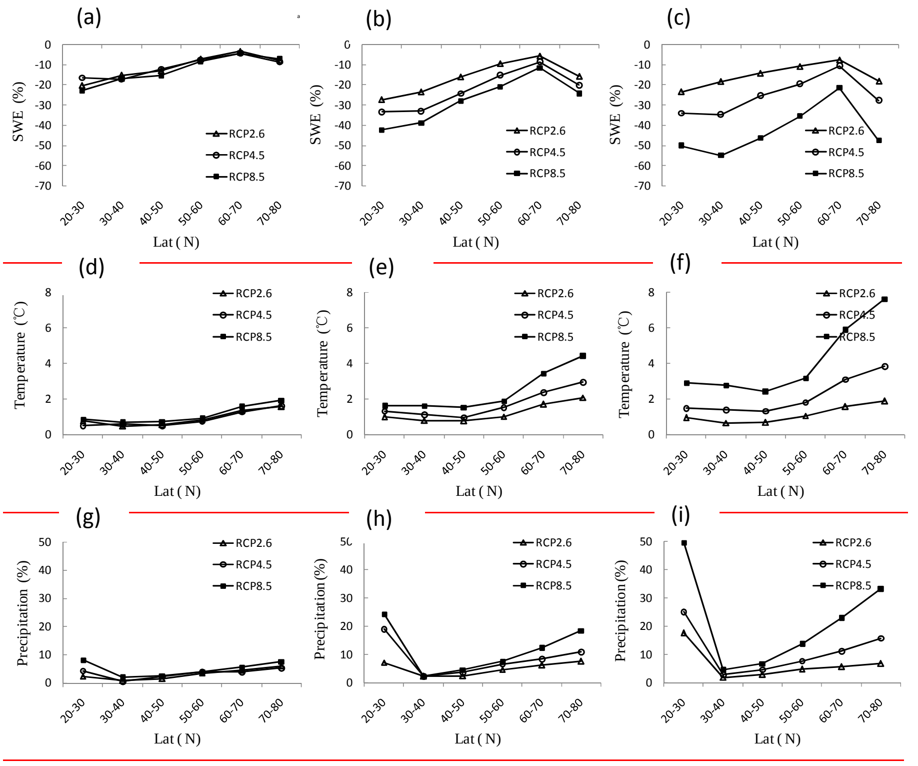

Figure 4. Relative zonal changes in mean annual SWE (a–c), mean annual air temperature (d–f) and mean annual precipitation (g–i) over Northern Hemisphere land for 2016−2035 (left), 2046−2065 (middle), and 2080−2099 (right) relative to the 1986−2005 reference period.

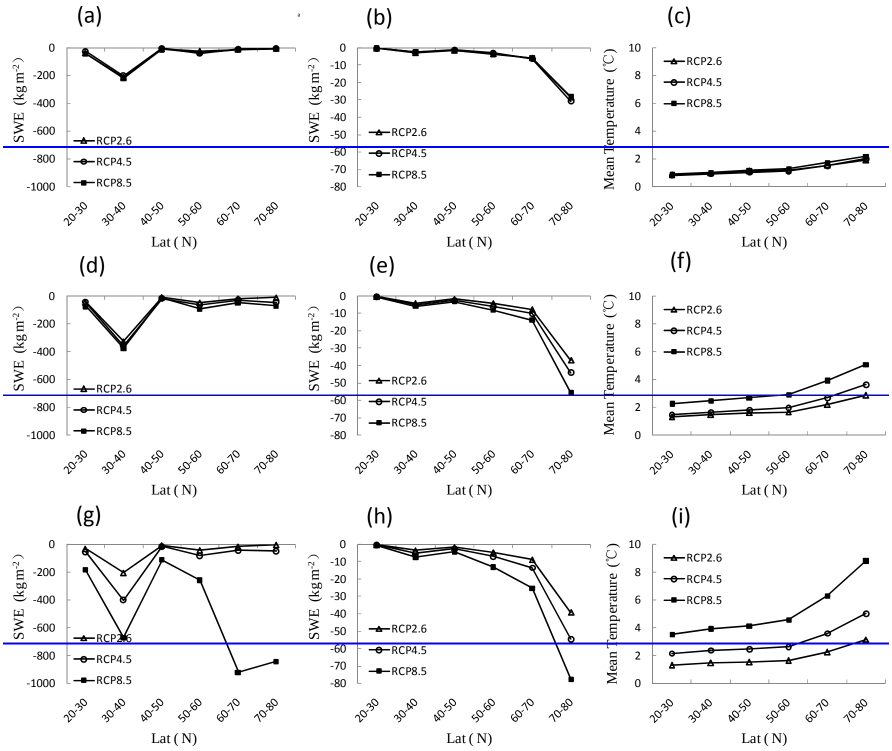

~~Figure. 4. Zonal changes in maximum annual SWE (panels a, d, g), mean annual SWE (panels b, e, h), and mean annual air temperature (panels c, f, i) for 2016–2035 (top), 2046–2065 (middle), and 2080–2099 (bottom), relative to the 1986–2005 mean.~~

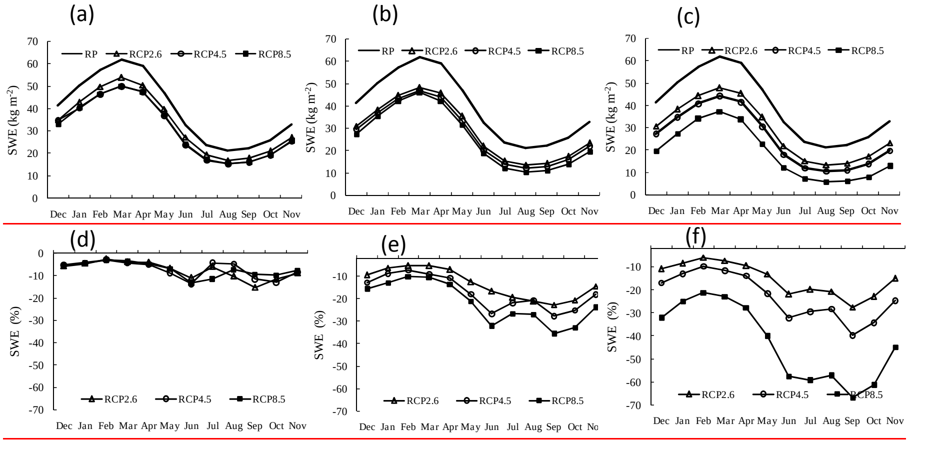

Figure 5. Projected monthly average (a–c) and relative change (RE) (d–f) in SWE over Northern Hemisphere land for 2016−2035 (left), 2046−2065 (middle), and 2080−2099 (right). Panels d–f show changes relative to the 1986−2005 reference period.

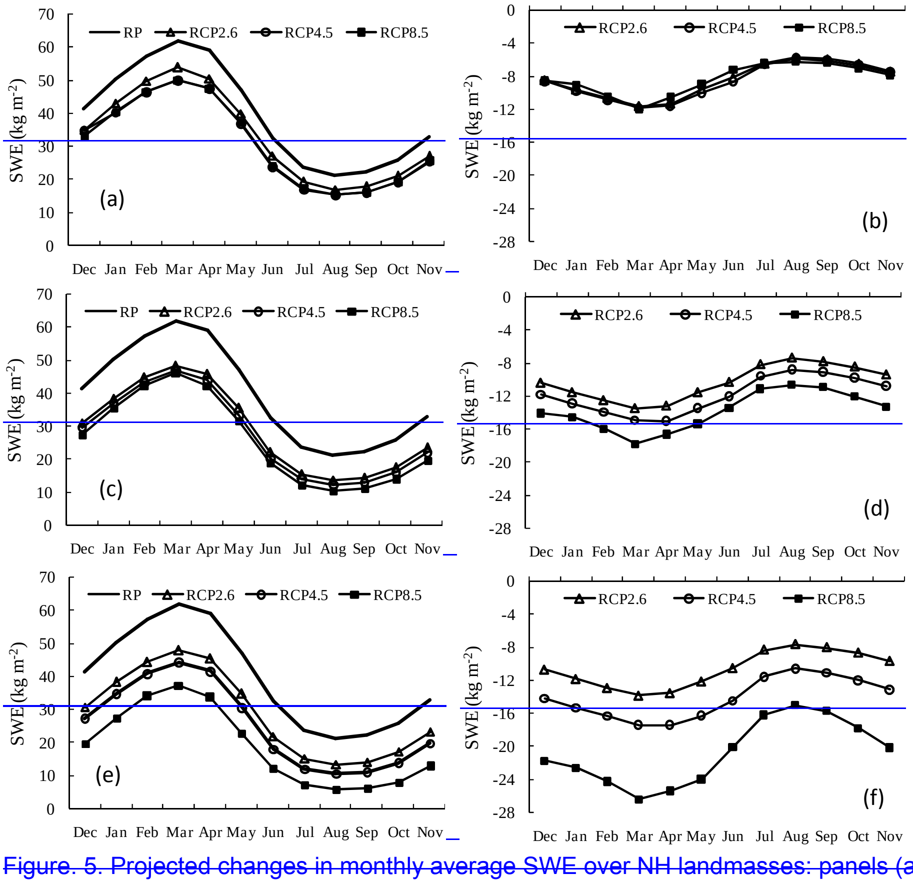

~~Figure. 5. Projected changes in monthly average SWE over NH landmasses: panels (a), (c), and (e) show the output of the RP (1986-2005), RCP2.6, RCP4.5, and RCP8.5 simulations; panels (b), (d), and (f) depict changes in SWE, relative to RP, for 2016–2035 (top), 2046–2065 (middle), and 2080–2099 (bottom).~~

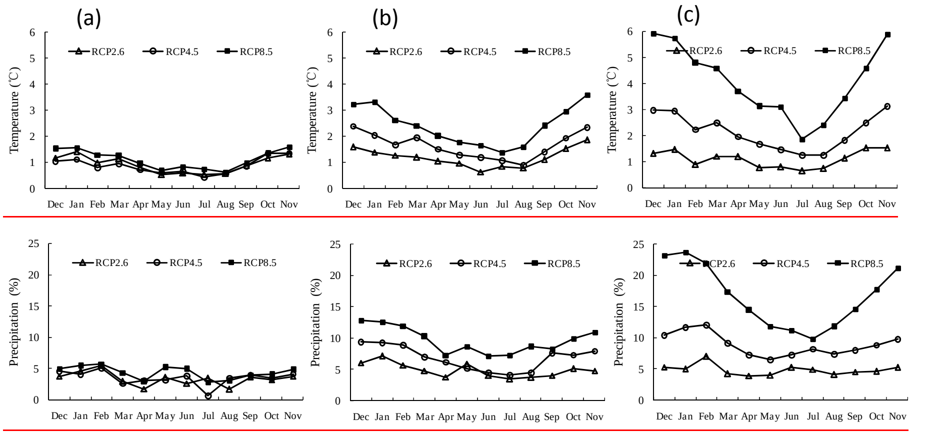

Figure 6. Changes in mean annual air temperature (a–c) and the relative change (RE) in precipitation (d–f) over Northern Hemisphere land for 2016−2035 (left), 2046−2065 (middle), and 2080−2099 (right) for three RCPs, relative to the 1986−2005 reference period.

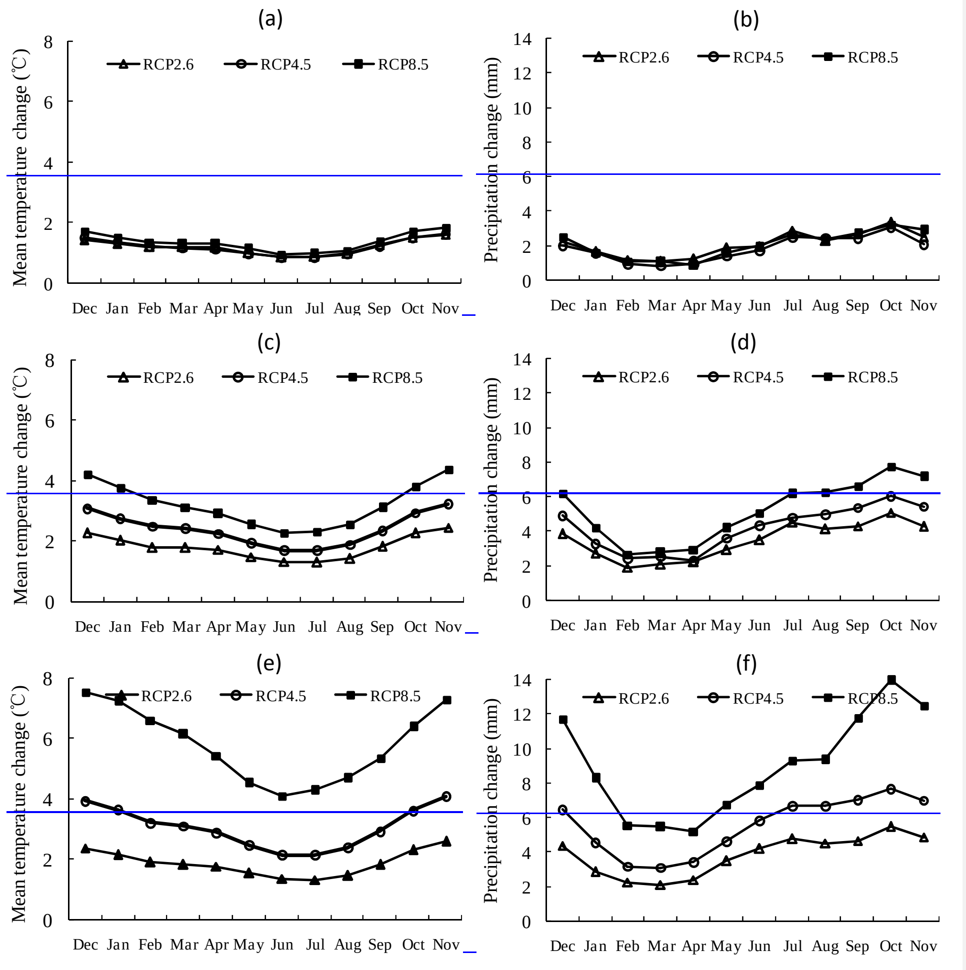

~~Figure. 6. Changes in mean annual air temperature (left) and precipitation (right) for 2016–2035 (a, b), 2046–2065 (c, d), and 2080–2099 (e, f), relative to the 1986–2005 mean, for three RCPs.~~

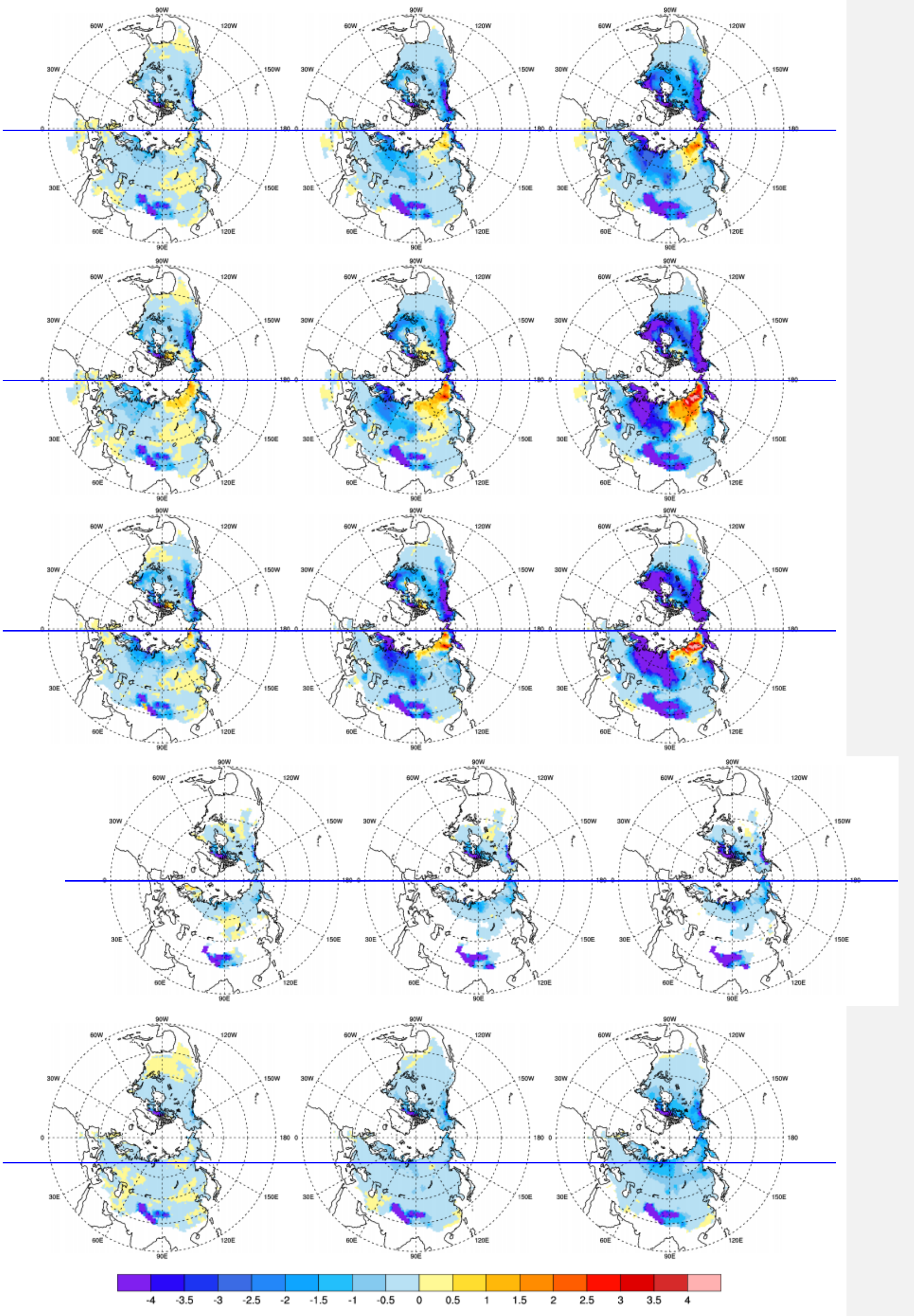
-4 -3.5 -3 -2.5 -2 -1.5 -1 -0.5 0 0.5 1 1.5 2 2.5 3 3.5 4

~~Figure. 7. Spatial distributions of projected SWE trends (kg m^{-2}/10a) between 2006 and 2099 for the three RCPs. Shaded areas represent regions where trends reach 95% significance. The five rows indicate the annual mean, winter, spring, summer, and autumn SWE. The three columns are RCP2.6, RCP4.5, and RCP8.5.~~

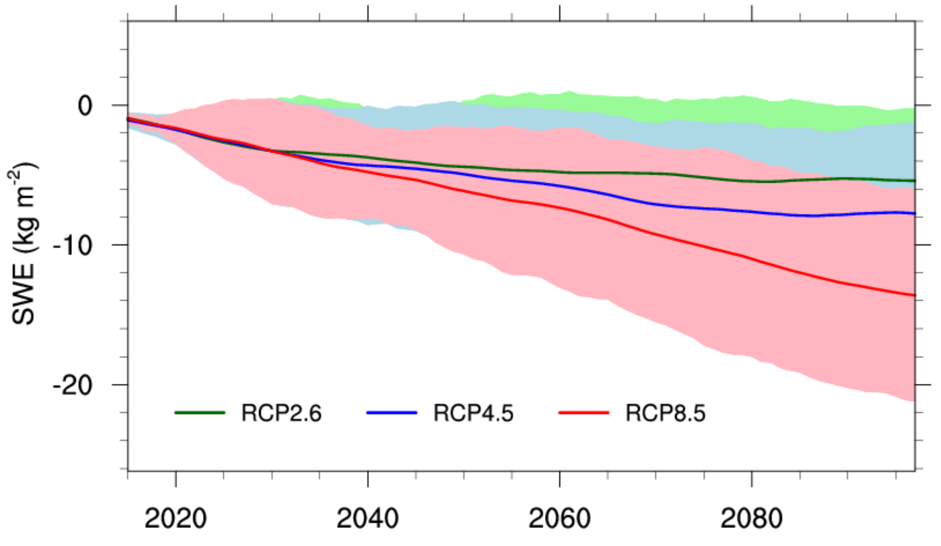

Figure. 7~~8~~. Projected changes in mean annual SWE over NH landmasses during 21st century~~, relative to RP (1986-2005),~~ for all three RCPs (green: RCP2.6; blue: RCP4.5; red: RCP8.5). The mean value for the 1986–2005 reference period is subtracted from all values. Also shown is the multi-model mean for all available models for each scenario. The 10-yr running average ~~is~~was derived for each model before calculation of the multi-model mean. Shaded areas denote the inter-model standard deviation for each ensemble mean.

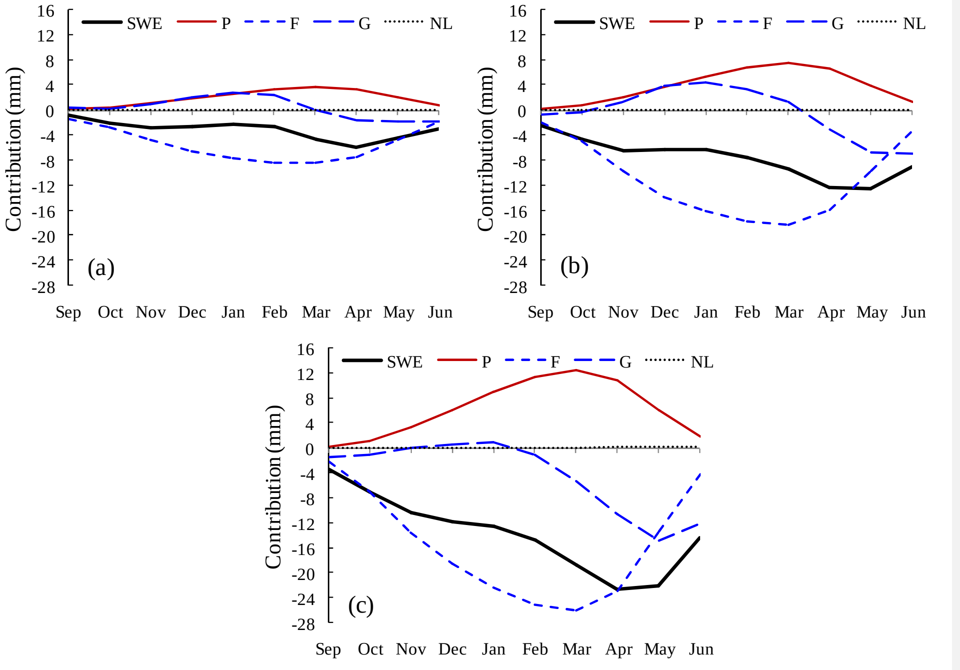

Figure 8. Mean changes in SWE decomposed using Equation (4) to show the contribution of changes in precipitation (ΔP), the fraction of solid precipitation (ΔF), the fraction of accumulated snowfall that remains on the ground (ΔG), and nonlinear terms (*NL*) during the period of 2016-2035 (a), 2046-2065 (b), and 2080-2099 (c) for RCP8.5, relative to the 1986–2005 reference period.

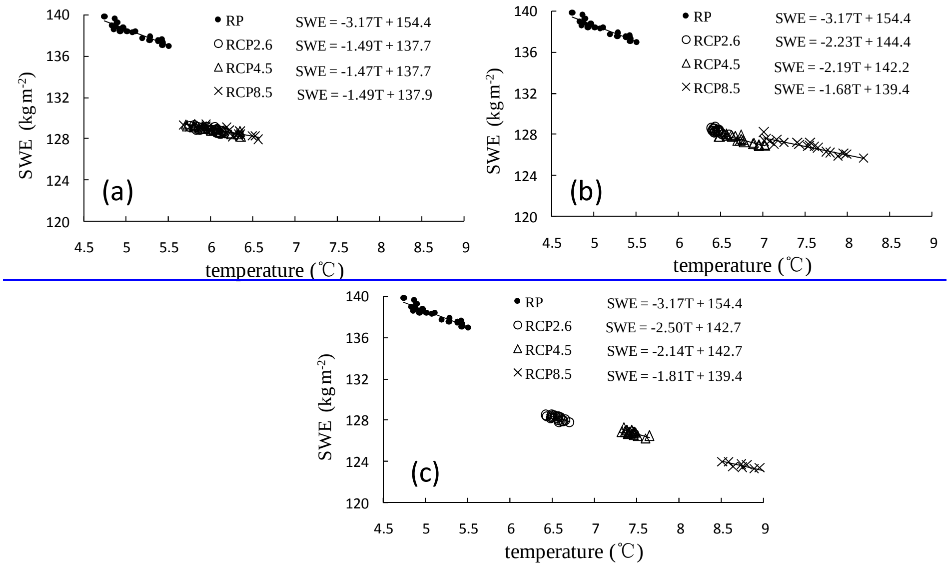

~~Figure. 9. Sensitivity of SWE to mean annual temperature over NH landmasses, derived from three RCPs, for the periods 2016−2035 (a), 2046−2065 (b), and 2080−2099 (c). The term 'RP' indicates the reference period of 1986−2005.~~